CARBON 50 (2012) 259–264

Available at www.sciencedirect.com

SciVerse ScienceDirect

journal homepage: www.elsevier.com/locate/carbon

Electron beam-induced formation and displacement of metal clusters on graphene, carbon nanotubes and amorphous carbon

O. Cretu [a], J.A. Rodríguez-Manzo [a], A. Demortière [b], F. Banhart [a,*]

[a] Institut de Physique et Chimie des Matériaux, UMR 7504 CNRS, Université de Strasbourg, 23 rue du Loess, 67034 Strasbourg, France
[b] Center for Nanoscale Materials, Argonne National Laboratory, 9700 S. Cass Ave., Argonne, IL 60439, USA

ARTICLE INFO

Article history:
Received 15 July 2011
Accepted 20 August 2011
Available online 25 August 2011

ABSTRACT

Nanocrystals of different metals with sizes of 2–6 nm are deposited on graphene, carbon nanotubes, or amorphous carbon films. Irradiation with a highly focused electron beam is used to split clusters of a few metal atoms (<1 nm in diameter) from the crystals. The metal clusters follow the electron beam spot on the graphitic surface when the beam is slowly deflected away from the clusters. This unusual behaviour of metals on graphitic surfaces is explained in terms of electron beam-induced activation of the graphitic surfaces and covalent bonding between metal and carbon atoms. The technique might be applicable in (sub-)nanometre structuring of graphene with metal dots.

1. Introduction

The interaction between graphene or carbon nanotubes (CNTs) and metals [1] is of high importance in the development of electronic devices. Metal–carbon contacts are necessary for connecting carbon devices with their periphery. Furthermore, metals inject charge into the electron system of graphene which shifts the Fermi level and may be used for doping. Metal atoms or metal layers on top of graphene are therefore a possibility to modify the properties of graphene, but for application in a nanodevice this has to be done with high lateral precision. However, before suitable metal–graphene composite systems can be made, a detailed understanding of the chemical interaction between graphene and different metals is necessary. The type of bonding, a possible transfer of charge, but also the mechanical robustness of the interface are important issues. While a perfect (non-defective) graphitic surface (graphene or CNTs) interacts weakly with metals by van der Waals interaction, the edges or defects with dangling bonds form much stronger covalent bonds with metals. An intermediate case is the arrangement of reconstructed defects in graphene [2] such as pentagon–heptagon combinations that interact with metals due to the modified pi-electron density around the defect [3,4]. After several studies of the metal–graphene interaction it became clear that graphene has to be activated to form bonds and so to interact sufficiently strong with metals. A technique of activation with ultimate lateral selectivity is electron irradiation with a focused electron beam. Recent *in situ* experiments have shown patterns created with sub-nanometre resolution [5].

Here we show that electron irradiation can induce the migration of small metal clusters over graphene, CNTs, or amorphous carbon surfaces. The focused electron beam in a transmission electron microscope (TEM) is used to split clusters of a few metal atoms from larger metal crystals. The clusters follow the electron beam spot when it is moved over the surface.

2. Experimental

Graphene samples were made by exfoliating natural graphite (NGS Naturgraphit GmbH) with regular Scotch tape [6]. After

* Corresponding author.
E-mail address: florian.banhart@ipcms.unistra.fr (F. Banhart).
0008-6223/$ - see front matter
doi:10.1016/j.carbon.2011.08.043

subsequent peeling steps, the tape was dissolved in acetone, and the resulting suspension was dropped on standard metallic (Mo and Ti) support grids for TEM. In order to improve the quality of the layers [7], the samples were annealed between 1000 and 2000 °C in an ultrahigh-vacuum furnace. Metal crystals were deposited on the layers either by adding a few drops of a colloidal nanocrystal solution (Pt, Pd) [8,9], by evaporation from hot filaments (Au, Fe, Co), or by evaporation from the metallic TEM grid during heating (Mo). Multiwall carbon nanotubes (MWNTs) were synthesized by aerosol pyrolysis [10,11] of the vapour from a hydrocarbon–organometallic solution. The solutions with 3 wt.% organometallic compound were atomized in the presence of Ar, and the resulting aerosol directed into a quartz tube furnace. The resulting MWNT material was scraped from the tube walls. The powders consisting of MWNTs and metal crystals were dispersed ultrasonically in ethanol and deposited onto standard copper grids for electron microscopy. Metal nanocrystals (Co, Pt or Au) were sputtered onto the surface of the MWNTs. Co and Pt wet the surface of the MWNTs [12] and form a layer, thus an annealing treatment was necessary to induce coalescence of the crystallites by ripening. As a third type of substrate, amorphous carbon films were used, under the form of standard holey carbon films of approximately 10 nm in thickness which are available commercially for electron microscopy (Agar Scientific).

In situ electron microscopy experiments were carried out by using a heating specimen stage in a scanning transmission electron microscope (STEM) with field emission source and a condenser with correction of the spherical aberration (Jeol 2100F). The size of the electron beam spot on the sample varied between 0.1 and 0.13 nm, which defines not only the image resolution in the STEM mode but also the scale for beam-induced structuring. The beam current density was around 10^5 A/cm^2. The images were taken in the high-angle annular dark-field (HAADF) mode, allowing a direct interpretation of the contrast and an easy differentiation between light and heavy atoms. The specimen temperature was varied between 20 and 500 °C in the microscope.

3. Results

The principle of the experiment is shown schematically in Fig. 1. When the electron beam spot was focused onto the edge of a metal crystal as shown in the STEM image in Fig. 2a, a small number of metal atoms was seen to split from the crystal (Fig. 2b). The metal atoms form a cluster whose size depends on the irradiation time. If the beam was slowly moved away from the large metal crystal, the cluster followed the beam spot and migrated over the graphene surface (Fig. 2c and d). During the migration of the cluster, some atoms remained on the trace of the cluster (visible in Fig. 2d). The same effect was also observed for CNTs. Fig. 3 shows the displacement of a Pt cluster over the surface of a CNT. The cluster has been split from the crystal on the left-hand side. The images show that the cluster's size becomes progressively smaller during its migration, owing to the loss of atoms along the way.

Each displacement experiment was performed over the course of a few (typically 2–3) minutes. The electron beam was moved away from the metal nanoparticle at a rate of roughly 1 nm/min. The migration speed of the metal atom clusters themselves appears to be high enough to follow the moving beam instantaneously. This is visible in Movie 1 for few-layer graphene and in Movie 2 for a CNT, which show typical step-by-step displacement processes.

The splitting of small clusters from larger metal particles did not show a measurable temperature effect between 20 and 500 °C. A certain minimum distance (for example, about 0.5 nm in the case of Pt) between the metal cluster and the electron beam spot is necessary for displacing the cluster, which does not depend on temperature either. The measurements are summarized in Fig. 4. Furthermore, no influence of the size of the initial metal particle on the split-

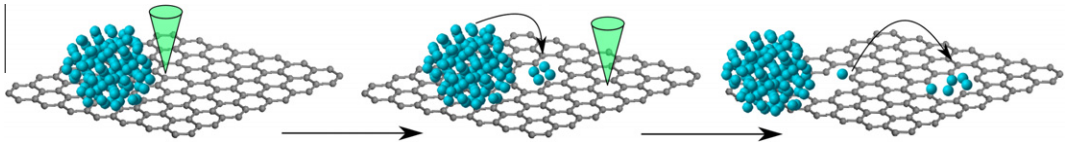

Fig. 1 – Principle of the experiment. The electron beam (cone) is focused onto the edge of a metal crystal. A metal cluster splits from the host crystal and follows the slowly moving electron beam over the graphene surface.

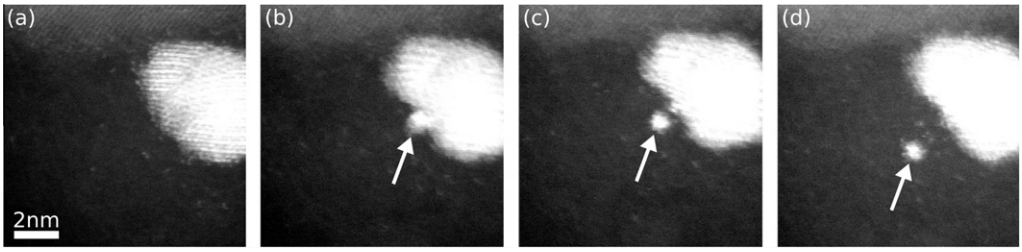

Fig. 2 – HAADF STEM images showing the displacement and migration of a Pt cluster (arrowed) on ~10-layer graphite at 200 °C. The images show the Pt crystal before (a), after the initial irradiation (b) and after further irradiation with an electron beam spot moving away from the particle (c,d). Individual atoms left behind the cluster can be seen in (d).

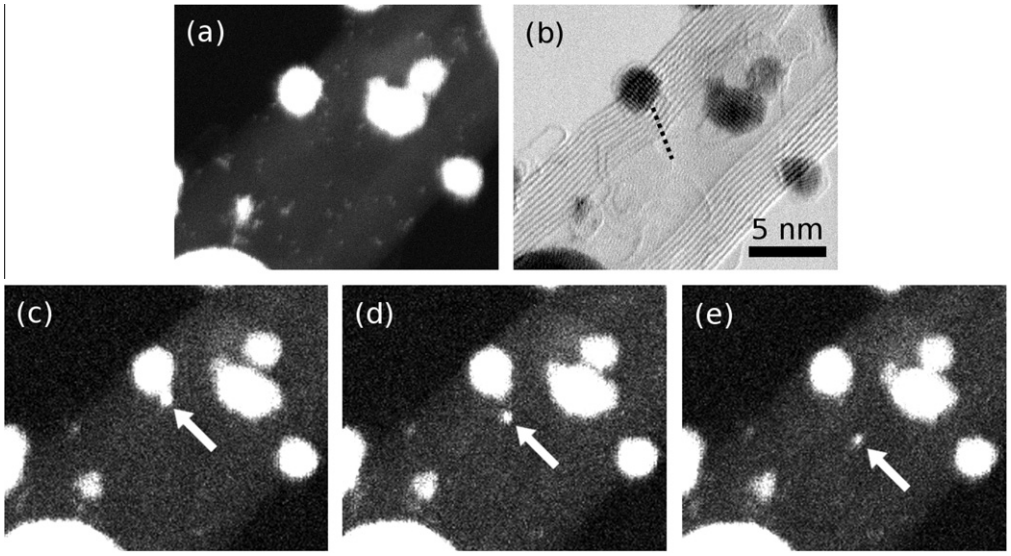

Fig. 3 – Displacement and migration of a Pt cluster over a MWNT. Dark (a) and bright-field (b) STEM images show the initial state of Pt particles on the MWNT (12 nm in diameter and 10 walls). The dotted line in (b) marks the path of the electron beam. (c–e) Dark-field images of the splitting and migration of the Pt cluster (~0.5 nm in diameter, arrowed).

ting mechanism was observable. Particles with sizes between 2 and 6 nm were studied; the average size is around 3 nm. The experiment is difficult with larger particles due to overhangs at the edges.

The process works for all metals that were deposited on carbon substrates in this study, *i.e.*, Fe, Co, Ni, Mo, Pd, Pt, and Au on graphene, Co, Pt, Au on CNTs, and Pt on amorphous carbon. However, some metals (for instance Mo) proved to be more resistant to irradiation, making it difficult to split off a cluster and thus requiring either higher irradiation doses or smaller distances between the particles and the beam.

It was found that the beam-induced displacement of metal clusters works on different types of carbon substrates. Fig. 5a shows the displacement and trapping of Au particles on single-layer graphene. The inset shows a bright-field STEM image where the graphene layer is visible. To verify that it is really a single layer, intensity profiles across graphene step edges in high-angle dark-field images were analyzed. Fig. 5b shows the displacement of Pd on a graphite substrate (approximately 10 graphene layers), this time carried out with lower electron beam energy (100 kV). Fig. 5c shows the same type of experiment on an amorphous carbon film (that could, however, graphitize locally under electron irradiation). At lower beam energies, a higher irradiation dose is necessary to displace the atoms, and long beam exposures are needed in order to achieve noticeable effects. However, experiments with non-carbon substrates such as crystalline silicon or amorphous silicon monoxide films were unsuccessful, and a beam-induced splitting or migration of metal clusters was not observable in these cases.

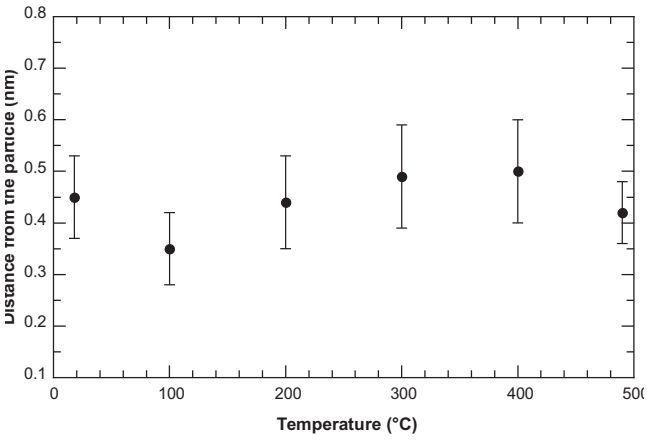

Fig. 4 – Maximum distance between the electron beam spot and the Pt nanoparticle for which the displacement of the cluster takes place, as a function of temperature.

Fig. 6 shows three Pt clusters that were split from the large Pt crystal nearby. The smallest one of them is only a few atoms in size, as estimated from the HAADF image (see inset of Fig. 6a). Another example is shown in Movie 3 where, after a few-seconds irradiation, a very small cluster of atoms leaves the particle. Such sub-nanometre precision was achieved due to the precise beam control in the STEM mode of the microscope.

Contamination effects are often observed during spot irradiation in the TEM and have recently been used to create patterns on graphene surfaces [13]. However, this can be excluded here because the phenomenon in our case does not depend on temperature. The typical contamination spots would not appear at high specimen temperature.

4. Discussion

It has recently been shown that thin metal layers can be grown on graphene or amorphous carbon by electron irradiation of the edge of metal crystals sitting on the carbon layer [14]. An explanation of this phenomenon has been given in terms of beam-induced activation of the carbon layer, leading to the trapping of mobile metal atoms on the irradiated carbon surfaces. The present observations could be based

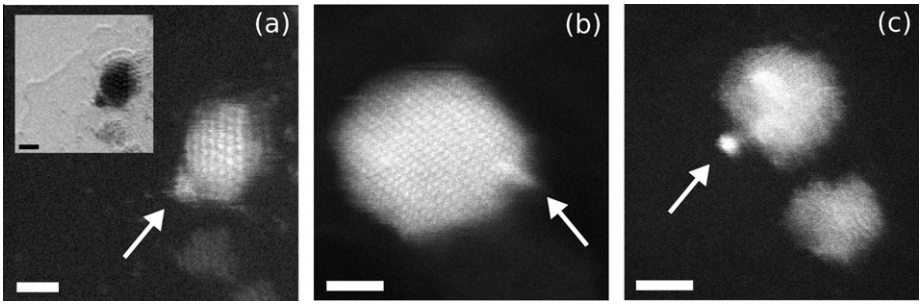

Fig. 5 – Splitting of metal clusters under different conditions. (a) Au on single-layer graphene at 475 °C (inset shows a bright-field image of the same area); (b) Pd on graphite at 400 °C, initiated with a 100 kV electron beam; (c) Pt on amorphous carbon at 300 °C. All scale bars are 2 nm.

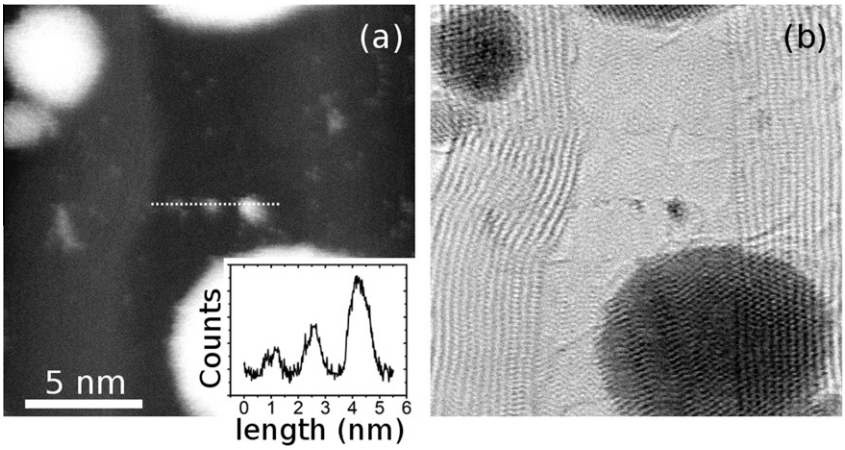

Fig. 6 – Dark (a) and bright-field (b) STEM images of three Pt clusters of different sizes that were split from the large Pt crystal. The inset of (a) shows the intensity profiles from the dotted line, which is proportional to the cluster mass.

on a similar process, but show a different behaviour of the metal. The electron beam is focused onto a spot of ~0.1 nm in diameter, leading to an extremely localized activation of carbon atoms and thus to the migration of metal clusters consisting of only a few atoms. This allows a patterning of graphene with metal dots with almost sub-nanometre precision. The technique applied here gives a similar lateral precision as the one published in [5], owing to the similar performances of the microscopes used for the experiments.

The splitting of metal clusters from larger crystals as it has been done here can be explained by the beam-induced surface mobility of metal atoms on the metal particles. The surface displacement rates are not the same in different metals, *e.g.*, less surface atoms are displaced in heavier elements [15]. Table 1 summarizes the threshold energies for bulk displacement [16] and surface sputtering [15] for all metals used in this study.

However, it must be taken into account that the mobility of the atoms on the metal surfaces can already be induced by lower electron energies than needed for sputtering. This is apparent as the electron energy in the experiment was 200 keV but heavy metal atoms (Mo, Pt, Au) are mobilized although their sputtering threshold energies are above electron energies of 200 keV. The available data in Table 1 should just be taken as reference values for comparing the elements among each other. Radiation-enhanced diffusion should therefore be considered as the likely mechanism leading to the mobility of surface atoms.

Table 1 – Threshold energies for displacing metal atoms in the bulk (T_b) and on the surface (T_s) by knock-on collisions with energetic electrons. T is the energy of the displaced metal atom and E denotes the corresponding beam electron energy. T_s was calculated according to Egerton et al. [15]; T_b was taken from Jung [16].

Element	Atomic mass	T_b [eV]	T_s [eV]	E_s [keV]
Fe	55.8	17	4.3	100
Ni	58.7	21	4.8	115
Co	58.9	23	4.7	115
Mo	95.9	27	6.8	240
Pd	106.4	34	3.8	160
Pt	195	34	5.8	380
Au	197	34	3	225

Once migrating, the metal atoms reach the carbon substrate and can be trapped there if metal–carbon bonds are formed. A condition is, however, that the carbon surface is reactive with dangling bonds, which is induced by electron irradiation. If the electron energy is above the displacement threshold of approximately 80–100 keV [17], carbon atoms

are displaced, leaving vacancies with dangling bonds. Double vacancies reconstruct and form arrangements of pentagonal and heptagonal rings by eliminating all dangling bonds, but the enhanced pi-electron density above these defects allows a bonding of metal atoms [3].

The small area under the beam just allows a few metal atoms to be trapped on the carbon surface. The localization of the trapped cluster depends on the energy of the respective metal–carbon bond [18]. It should be noted that the process works even for atoms such as Au which are known to form weak bonds with carbon (previous attempts to create metal–CNT junctions had proven unsuccessful for noble metals [19]). The process does not work on other surfaces, *e.g.*, Si or SiO, as it is shown here, due to the absence of sufficiently strong bonding with metal atoms. It has also to be taken into account that an electron energy of 200 keV is not sufficient to create defects with dangling bonds in silicon. Due to the high electrical conductivity of the carbon substrates (graphene, CNTs, amorphous carbon film), charge effects should be negligible.

The fact that the metal clusters do not remain localized but follow the moving electron beam spot points to an annealing effect in the carbon layer. This is surprising because metal–carbon bonds have to be broken during the migration of the metal particles, and a restructuring of the carbon film is necessary. Both processes need activation energies of the order of 7 eV [18] which cannot be surmounted thermally at the temperatures of the experiments, but electron irradiation can supply at least part of the activation energy. On the other hand, metal atoms are left in the trace of the moving cluster as can be seen in Fig. 2d, showing that a complete restructuring of the carbon film does not take place. As another type of bonding between metal atoms and graphitic substrates, the trapping of metal atoms on reconstructed multiple vacancies [3] should be considered. The metal–carbon bonding energy is only around 2 eV and, thus, much weaker in this case, but allows a successive de-trapping of metal atoms from the defects.

5. Conclusions

To conclude, we have shown that it is possible to split and displace metal clusters with diameters of less than 1 nm from larger metal particles (2–6 nm) on graphenic or amorphous carbon substrates. The beam-induced activation of carbon allows us to place small metal clusters in pre-defined locations. The guiding of metal clusters on a graphene surface by a focused electron beam is an unexpected phenomenon but might be the basis of different applications. It can be used for patterning graphene or CNTs with metal dots and creating a system of metal islands. This would change the electronic properties of graphene. The phenomenon might also be used for tailoring the size of metal islands on graphene.

Acknowledgements

Funding by the Agence Nationale de la Recherche ANR (NANOCONTACTS, NT09 507527) is gratefully acknowledged. The authors thank M. Acosta, F. Scheurer, and G. Schull for supplying specimen material.

Appendix A. Supplementary data

Supplementary data associated with this article can be found, in the online version, at doi:10.1016/j.carbon.2011.08.043.

REFERENCES

[1] Banhart F. Interactions between metals and carbon nanotubes: at the interface between old and new materials. Nanoscale 2009;1:201–13.
[2] Banhart F, Kotakoski J, Krasheninnikov AV. Structural defects in graphene. ACS Nano 2011;5(1):26–41.
[3] Cretu O, Krasheninnikov AV, Rodríguez-Manzo JA, Sun L, Nieminen R, Banhart F. Migration and localization of metal atoms on graphene. Phys Rev Lett 2010;105: 196102 (19).
[4] Rodríguez-Manzo JA, Cretu O, Banhart F. The trapping of metal atoms in lattice vacancies in graphene and carbon nanotubes. ACS Nano 2010;4(6):3422–8.
[5] van Dorp WF, van Someren B, Hagen CW, Kruit P, Crozier PA. Approaching the resolution limit of nanometer-scale electron beam-induced deposition. Nano Lett 2005;5(7): 1303–7.
[6] Novoselov KS, Geim AK, Morozov SV, Jiang D, Zhang Y, Dubonos SV, et al. Electric field effect in atomically thin carbon films. Science 2004;306(5696):666–9.
[7] Liu Z, Suenaga K, Harris PJF, Iijima S. Open and closed edges of graphene layers. Phys Rev Lett 2009;102(1): 015501.
[8] Demortière A, Launois P, Goubet N, Albouy PA, Petit C. Shape-controlled platinum nanocubes and their assembly into two-dimensional and three-dimensional superlattices. J Phys Chem B 2008;112(46):14583–92.
[9] Demortière A, Petit C. First synthesis by liquid–liquid phase transfer of magnetic Co_xPt_{100-x} nanoalloys. Langmuir 2007;23(16):8575–84.
[10] Kamalakaran R, Terrones M, Seeger T, Kohler-Redlich Ph, Rühle M. Synthesis of thick and crystalline nanotube arrays by spray pyrolysis. Appl Phys Lett 2000;77(21):3385–7.
[11] Mayne M, Grobert N, Terrones M, Kamalakaran R, Rühle M, Kroto HW, et al. Pyrolytic production of aligned carbon nanotubes from homogeneously dispersed benzene-based aerosols. Chem Phys Lett 2001;338(2–3):101–7.
[12] Zhang Y, Nathan FW, Robert CJ, Dai H. Metal coating on suspended carbon nanotubes and its implication to metal–tube interaction. Chem Phys Lett 2000;331(1): 35–41.
[13] Meyer JC, Girit CO, Crommie MF, Zettl A. Hydrocarbon lithography on graphene membranes. Appl Phys Lett 2008;92:123110 (12).
[14] Rodriguez-Manzo JA, Banhart F. Electron beam-induced nanopatterning of multi-layer graphene and amorphous carbon films with metal layers. Appl Phys Lett 2011;98:183105 (18).
[15] Egerton RF, Li P, Malac M. Radiation damage in the TEM and SEM. Micron 2004;35(6):399–409.
[16] Jung P. Production of atomic defects by irradiation. In: Ullmaier H, editor. Atomic defects in metals, Landolt-Börnstein: Numerical data and functional relationships in science and technology, vol 25, Berlin; Springer; 1991 p. 1–87.

[17] Smith BW, Luzzi DW. Electron irradiation effects in single wall carbon nanotubes. J Appl Phys 2001;90:3509 (7).
[18] Krasheninnikov AV, Lehtinen PO, Foster AS, Pyykkö P, Nieminen RM. Embedding transition-metal atoms in graphene: structure, bonding, and magnetism. Phys Rev Lett 2009;102:126807 (12).
[19] Rodríguez-Manzo JA, Banhart F, Terrones M, Terrones H, Grobert N, Ajayan PM, et al. Heterojunctions between metals and carbon nanotubes as ultimate nanocontacts. PNAS 2009;106(12):4591–5.